# RELATION BETWEEN THE COMPTON PROFILE AND THE FERMI SURFACE IN ALUMINUM

R. A. Tawil*

**الخلاصة**

نقدم في هذا المقال نتائج حساب بطريقة الدفع التقريبية لتباين الخواص المحورية لمقطع الجانبي الكومبيتون ( Compton ) للألومونيوم .

وقد وجدنا أن هيكل هذا التباين مرتبط بطبولوجية سطح فيرمي ( Fermi ) وأن مقداره متعلق كيفاً بمساحة المقطع العرضي للمدارات على سطح فيرمي .

**ABSTRACT**

The anisotropy in the Compton profile of aluminum has been calculated by the Impulse approximation. The structure in the anisotropy is related to topology of the Fermi surface, and its magnitude is qualitatively related to the cross-sectional area of the orbits on the surface.

## INTRODUCTION

The single particle momentum density of an electronic system is an interesting and important physical quantity to study. It is very sensitive to the distribution of the valence electrons, incorporates such many-body effects as electron-correlation, and reflects the anisotropy in the charge distribution of the system. Also, under certain conditions to be presented shortly, the full one-dimensional profiles for this quantity can be measured directly by high energy Compton scattering experiments. This experimentally observable function of a single variable is termed the Compton profile (CP). In this paper, the anisotropy in the CP of aluminum along the three crystallographic directions is investigated and an attempt is made to qualitatively relate the structure in the anisotropy to the topology of the Fermi surface. This work may be regarded as a supplement to a recent report of a calculation of the CP in this metal[1], and follows a similar approach to that used for nickel[2].

Consider the process of Compton scattering of energetic photons by bound electrons. The intensity distribution profiles of the scattered photons may be related to the ground state momentum distribution of the scatterers if the following assumptions are made: (i) a non-relativistic independent-particle description is used for the dynamics of the electrons; (ii) the final states of the recoil electrons are single plane waves; and (iii) the binding energies of the electrons are small compared to the energy transfers from the photon to the electrons. Assumption (iii) constitutes the Impulse Approximation (IA) [3]. One also might want to eliminate multiple scattering or correct for it, and ascertain that the probability of a photon interacting with any particular electron is independent of that electron's momentum.

Let $\vec{p}$ denote the initial momentum of an electron in the system under study; $\vec{k}$, the change in the momentum after a Compton scattering event has occurred; and $\omega(\hbar=1)$, the energy transferred to the electron. Then the intensity of the scattered radiation observed along some fixed direction $\hat{x}$ in the solid, is proportional to

$$J_{\hat{x}}(q) = \frac{\Omega}{(2\pi)^3} \int d^3p\, P(\vec{p})\, \delta(q-\hat{x}.\vec{p}). \qquad (1)$$

in which P(p) is the momentum distribution

$\vec{k} = \frac{\vec{k}}{|\vec{k}|}$, $\Omega$ is the volume of the Wigner-Seitz cell,

and $q = m\omega/|\vec{k}| - \frac{1}{2}|\vec{k}|$ (2)

*Department of Physics, University of Petroleum and Minerals, Dhahran, Saudi Arabia

Equation (1) indicates that for a given direction $\hat{\chi}$, the CP, $J\hat{\chi}(q)$ is proportional to the integral of the momentum density in a plane perpendicular to $\hat{\chi}$ displaced from the origin by q. Alternatively, all electrons with a momentum component equal to q along $\hat{k}$ will contribute to this quantity.

In an independent electron model, the shape of $J\hat{\chi}(q)$ is determined mainly by the momentum-space electronic wave functions and by the Fermi surface topology. The Fermi surface determines the occupancy assigned to the quasi-particle states and can produce sharp structure on the otherwise relatively smooth q-dependence of the electron wave functions in this space [2, 4-6]. For most systems, the Fermi surfaces are not spherical and thus the occupancy effects introduce anisotropies in the CP. These anisotropies have been measured in the case of nickel [7,8]. At the present time, no such direct measurements have been reported on aluminium.

The wave functions that are used in this investigation have been generated in a band structure calculation[9]. The method of the band calculations utilizes a fully self-consistent modified-tight-binding scheme in a variational approach to the solution of the one-electron Schrodinger equation. Detailed accounts of the method have been published elsewhere [9-12] and will not be elaborated here.

The mathematical background necessary for the current investigation is displayed in the following section. In Section 3, the results are presented and discussed.

## 2. PROCEDURE

In the tight-binding method, the wavefunction for a state of wavevector g in band n, $\psi_n(\vec{g},\vec{r})$, is expanded in a set of localized orbitals (Wannier functions) $U_i(\vec{r})$ according to:

$$\psi_n(g,r) = \left(\frac{1}{N}\right)^{1/2} \sum_i \sum_\mu C_{ni}(\vec{g}) \exp(i\vec{g}.\vec{R}\mu)\, U_i(\vec{r}-\vec{R}_\mu), \quad (3)$$

where the $C_{ni}$'s are contraction coefficients determined self-consistently as described in reference 9. $\vec{R}_\mu$ is a direct lattice vector marking the site about which the $U_i$ is localized.

The counterpart of Eq. (3) in momentum space may be expressed as

$$\psi_n(\vec{g},\vec{p}) = \sum_i \sum_s C_{ni}(\vec{g})\, \delta_{\vec{g},\vec{p}-\vec{K}_s}\, \chi_i(p), \quad (4)$$

with

$$\chi_i(p) = \left(\frac{1}{\Omega}\right)^{1/2} \int \exp(-i\vec{p}.\vec{r})\; U_i(\vec{r})d^3r, \quad (5)$$

and $\vec{K}_s$ is a reciprocal lattice vector.

At $T=0^0k$, the momentum charge density can be written

$$P(\vec{p}) = \sum_{ng} \theta(E_f-E_n(\vec{g}))\, |\psi_n(\vec{g},\vec{p})|^2, \quad (6)$$

where $E_f$ is the Fermi energy, $E_n(\vec{g})$ is the energy of a state, and $\theta$ is a unit step function.

$\theta(x) = 1$ if $x \geq 0$,
$\theta(x) = 0$ if $x < 0$.

Substituting Equation (4) into Equation (6):

$$P(p) = \sum_{n,\vec{g}} \theta(E_F-E_n(\vec{g}))\, \Big|\sum_{i,s} C_{ni}(\vec{g})\delta_{\vec{p},\vec{g}+\vec{K}_s}\, \chi_i(\vec{p})\Big|^2,$$

$$= \sum_{n,\vec{g},\vec{s}} \theta(E_F-E_n(\vec{g}))\delta_{\vec{p},\vec{g}+\vec{K}_s} \sum_i C_{ni}(\vec{g})\, \chi_i(\vec{p})\Big|^2$$

$$= \sum_{n,\vec{g},\vec{s}} \theta(E_F-E_n(\vec{p}-\vec{K}_s)) \sum_i C_{ni}(\vec{g})\, \chi_i(\vec{p})\Big|^2 . \quad (8)$$

Equation (8) explicitly indicates that $\vec{p}$ lies outside the Brillouin zone, and as far as the step function is concerned the value of $\vec{p}$ is brought back into the zone by subtracting the appropriate $\vec{K}_s$. This cannot be done with $\chi_i(\vec{p})$, which must be considered for all p.

Equation (8) is substituted into (1) to give:

$$J\hat{\chi}(q) = \frac{\Omega}{(2\pi)^3} \sum_{n,\vec{g},\vec{s}} \int d^3p\, \theta(E_F-E_n(\vec{P}-\vec{k}_s))\, \delta(q-\hat{\chi}.\vec{p})$$
$$\times \Big|\sum_i C_{ni}(\vec{g})\, \chi_i(\vec{p})\Big|^2 . \quad (9)$$

In order to gain some insight into equation (9), the CP of the core bands will be considered first. Figure 1 displays the results for the three crystallographic

directions in aluminum. For these bands, the occupation numbers are always unity (i.e. in Equation 9 the step function is set equal to unit) and the CP is a smooth function of q. For the valence bands the corresponding results are displayed in Figure 2. In this figure the "occupancy effects" cause the discontinuity in the slope of the CP at $q_F$. Specifically, imagine the infinite p-space to be partitioned into regions which are repetitions of the Brillouin zone centered at reciprocal lattice points $\vec{K}_s$. The representation of the Fermi surface will now be the one in the extended zone scheme. Denote $\vec{p}.\hat{x}$ by $p_{\|}$, and the remaining components by $p_{\perp}$. Then the integration over $p_{\|}$ in Equation 9 can be done immediately to yeild:

$$J_k(q) = \frac{\Omega}{(2\pi)^3} \sum_{g,n,s} \int d^2 p_{\perp} \, \delta(E_F - E_n(p_{\perp} - K_{s_{\perp}}, q - k_{s_{\|}})$$

$$x \left| \sum_i C_{ni}(\vec{g}) \chi_i(p_{\perp}, q) \right|^2 \qquad (10)$$

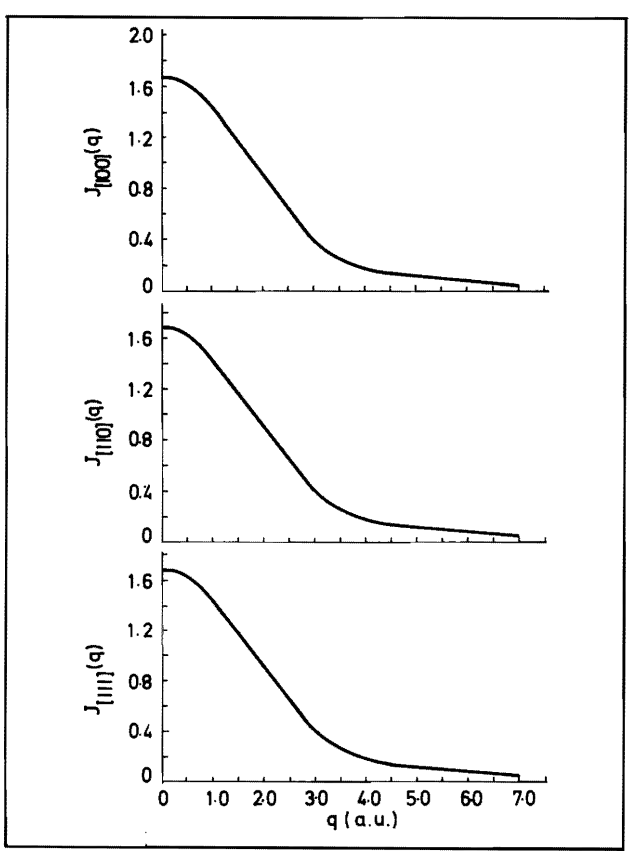


*Figure 1 : Core-electrons contribution to the Compton profile of Aluminium.*

In equation (10), whenever a plane perpendicular to $\hat{x}$ at a distance q from the origin is tangent to any of these repeated Fermi surfaces, structure is to be expected in $J\hat{x}$ (q). The amplitude of this structure will not be the same in each case because of the presence of $|\chi_i|^2$ is expected to decrease with increasing q in order to remain square integrable.

The actual computation of $J\hat{x}(q)$ employed wavefunctions expressed as linear combination of Gaussian-Type Orbitals. The numerical methods are the same as described in Reference [1]. In the next section the modifications introduced on the method will be presented and the results will be discussed.

## 3. RESULTS

For each set of the values reported in Table 4 of Reference[1], a fit utilizing Generalized Orthogonal Polynomials [13] of degree 6 was effected. The tolerance accepted in the fit was $10^{-5}$ which assured that the results in Table 1 are correct to the number of significant figures reported. The last column of this table includes the values obtained for the average CP which was approximated by the zeroth order in a six-degree Kubic Harmonic expansion.

Figure 3 is presented in order to display the agreement between the theoretical and experimental results [14,15]. The anisotropy in the CP for crystalline aluminium is presented in Figure 4.

The features in the anisotropy curves can be naturally subdivided into five regions. In the region for $q > 1.00$ a.u., no appreciable anisotropy is displayed. The slight anisotropies are due to the $\psi_1$ orbit on the Fermi surface [16] which is a second zone orbit. Examination of the entries in Tables 4 and 5 of Reference [9] is recommended at this stage.

The second region is bounded by $0.8 < q < 0.97$ a.u. This anisotropy is definitely resulting from the $\psi_1$ orbit which has the following dimensions:

$$\Gamma - X = 0.905 \text{ a.u.} \; ; \; \Gamma - W = 0.967 \text{ a.u.} \; ; \; \text{and } \Gamma - K = 0.831 \text{ a.u.} \qquad (9)$$

The structure in this region is the most prominent and is about 3.5% of $J\hat{x}(0)$. The reasons that this structure

has not been observed experimentally are first, that it occurs at the discontinuity in the CP curves (Figure 3), and second, that the experimental resolution with the present techniques is of the same order the agreement between the two experimental measurements [14,15] is about 3% in this region.

The region for q values between $0.28<q<0.62$a.u can be subdivided into two subregions; the first is that subregion which corresponds to $0.28<q<0.42$a.u., resulting from the $\xi$ orbit with dimensions 0.376 a.u., 0.281 a.u. and 0.417 a.u. in the[100],[110]and[111]directions respectively. The second subregion results from the $\gamma_5$orbit. Since the dimensions of the $\gamma_5$ orbit overlap those of the $\zeta$, the amplitude in the anisotropy for the $0.28<q<0.42$ a.u. region would be larger than that in the $0.42<q<0.62$ a.u.

Noting that the $\gamma_5$ orbit is "ellipsoidal" (see figure 5) with a large eccentricity, the anisotropy in the $0.0<q<0.28$ a.u. region is derived from this orbit and particularly from its cross-section in the (110) plane.

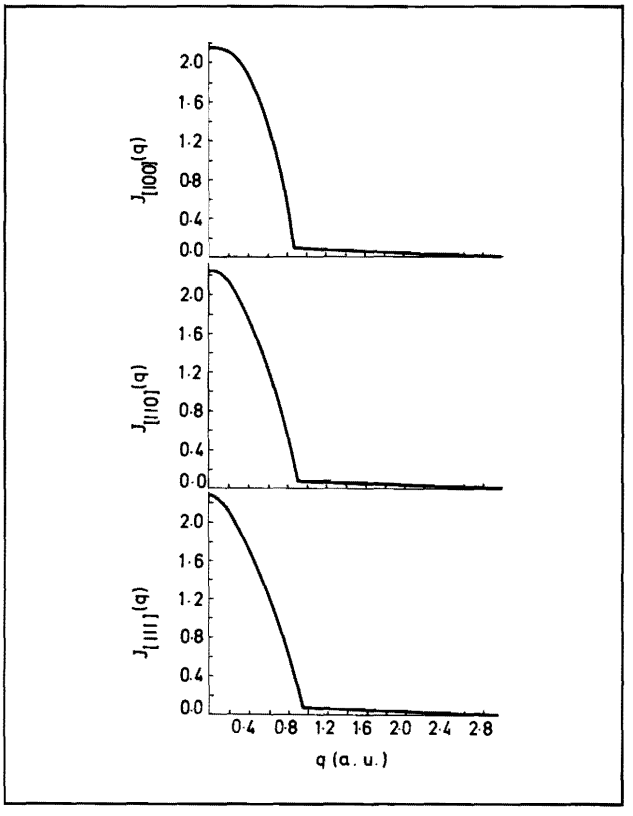


*Figure 2 : Valence-electrons contribution to the Compton profile of Aluminium.*

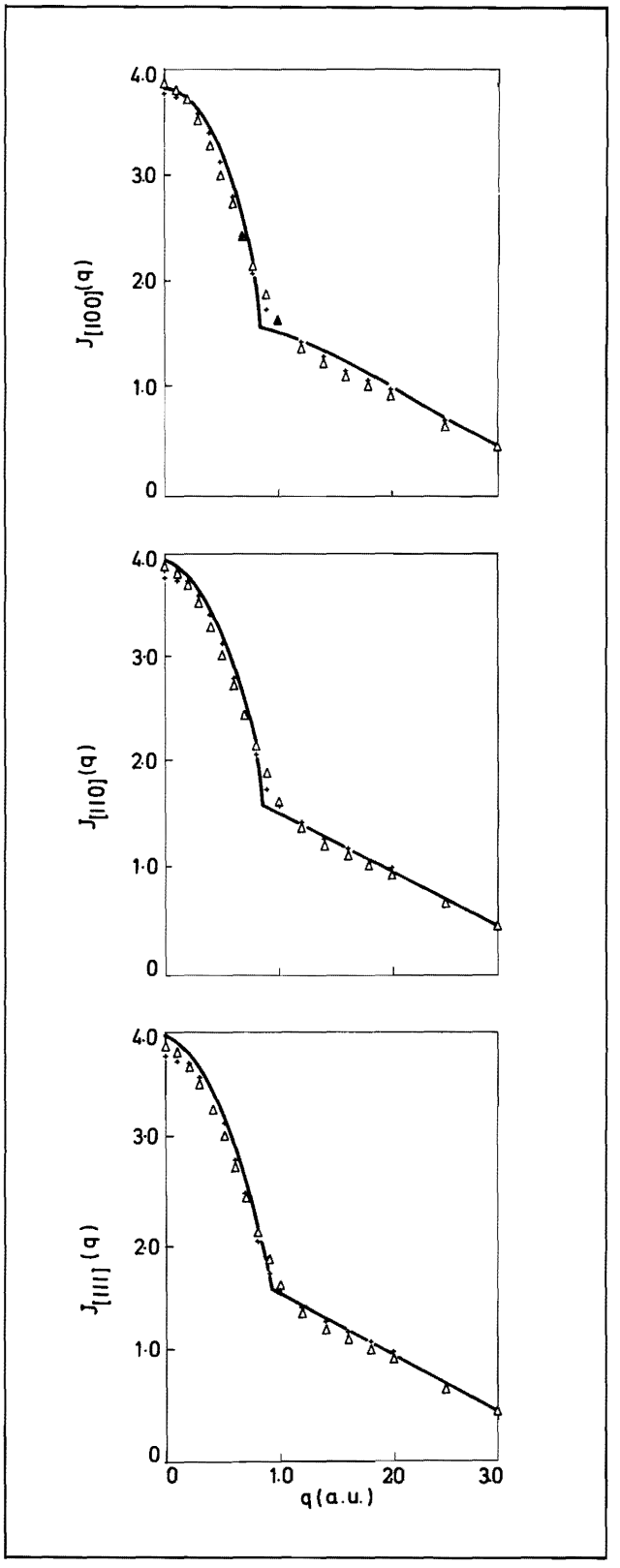


*Figure 3 : Total compton profile (excluding $1s^2$ - like band) of aluminium. △ results of Manninen et al. (Reference 14). + results of Cooper et al. (Reference 15).*

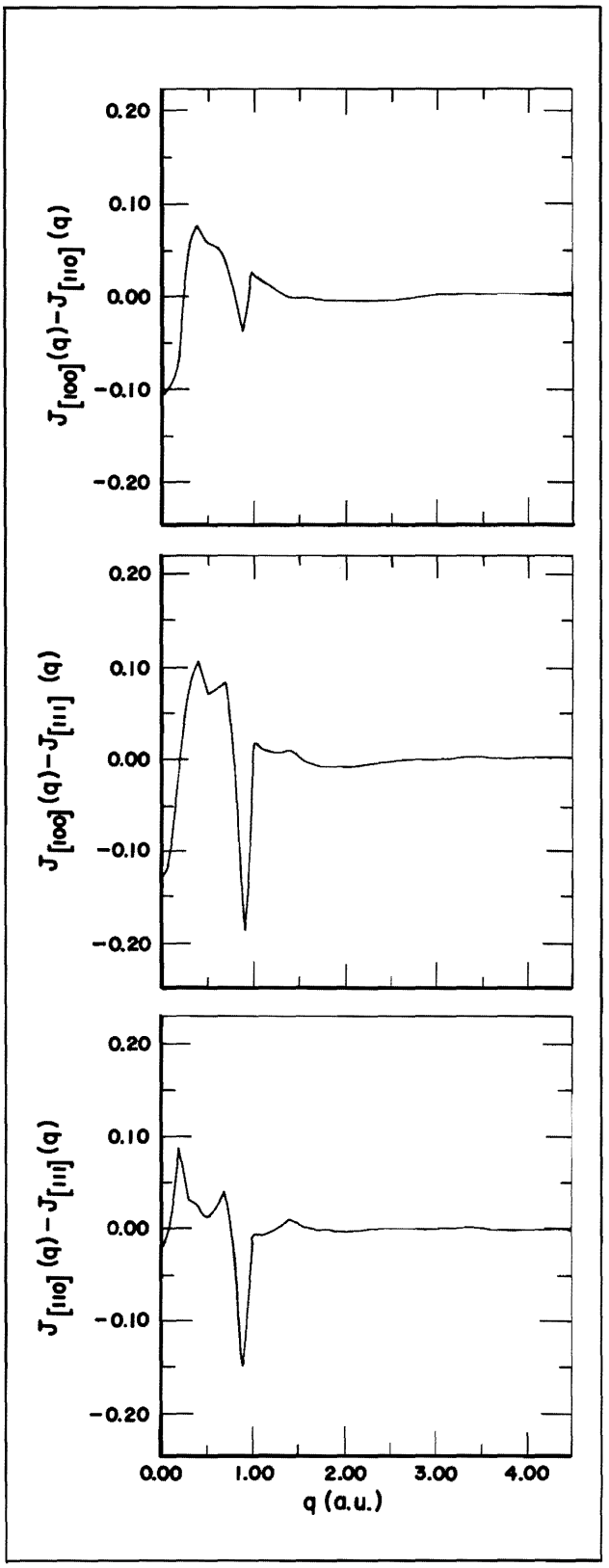


*Figure 4 : Calculated anisotropy in the Compton Profiles of aluminium.*

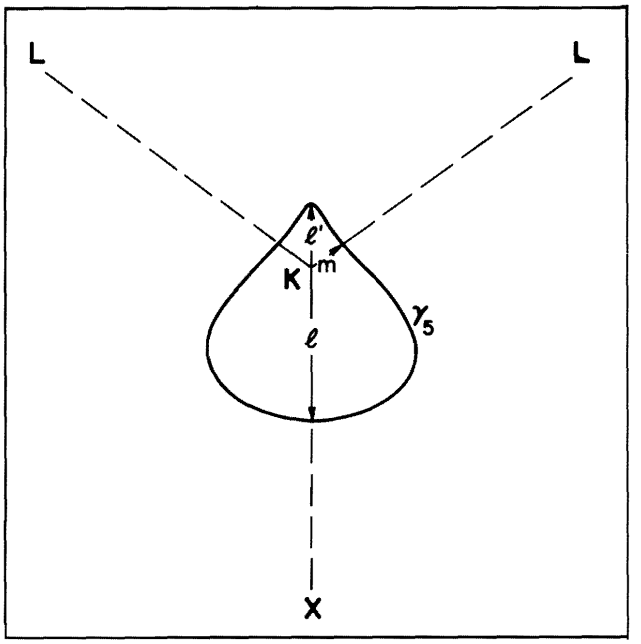


*Figure 5 : $\gamma_5$ orbit cross section in the (111) plane.*

Granted that the $J_{\hat{x}}(q)$ is proportional to the area of the cross-section of the Fermi surface in the plane perpendicular to $\hat{x}$, the analysis displayed above lends itself also to explaining the relative amplitudes of the anisotropy in the various regions. The anisotropy due to the $\psi_1$ orbit is the largest since the $\psi_1$ orbit encloses the largest cross-sectional area. Similarly one expects the amplitude (excluding the superposition effect) in the region $0.28<q<0.42$ a.u. to be intermediate to that with $0.0<q<0.28$ a.u. and $0.42<q<0.62$ a.u. The $\gamma_5$ orbit consists of 6 electron-pockets, the $\xi$ orbit consists of 4. Each of the units in the two orbits encloses approximately the same area.

## SUMMARY

In this paper it has been demonstrated that the Compton profiles in crystalline aluminium are anisotropic and that this anisotropy is intimately related to the topology of the Fermi surface and the cross sectional area of its orbits. It is also found that this anisotropy is small to be measurable by the present techniques. Experimental measurements with increased resolution should reveal the additional structure associated with the Fermi surface. Such measurements on the CP may enable determinations of alloy Fermi surfaces under circumstances in which de Haas-Van Alphen and related measurements are not possible.

The author acknowledges the opportunity extended to him by Battele Columbus Laboratories where the major computational portion of the calculation was performed, and thanks Professor C.W. Kern for his hospitality.

TABLE I

Total Compton profile of aluminum including the contribution from the $1s^2$ band.

| q | J [100] | J [110] | J [111] | <J> |
|---|---|---|---|---|
| 0.000 | 3.958 | 4.066 | 4.089 | 4.041 |
| 0.100 | 3.945 | 4.043 | 4.032 | 4.012 |
| 0.200 | 3.919 | 3.988 | 3.900 | 3.945 |
| 0.300 | 3.816 | 3.766 | 3.736 | 3.772 |
| 0.400 | 3.653 | 3.757 | 3.547 | 3.590 |
| 0.500 | 3.384 | 3.326 | 3.315 | 3.339 |
| 0.600 | 3.092 | 3.038 | 3.016 | 3.047 |
| 0.700 | 2.718 | 2.676 | 2.634 | 2.678 |
| 0.800 | 2.261 | 2.555 | 2.272 | 2.261 |
| 0.900 | 1.705 | 1.746 | 1.909 | 1.776 |
| 1.000 | 1.550 | 1.626 | 1.635 | 1.635 |
| 1.200 | 1.537 | 1.527 | 1.531 | 1.531 |
| 1.400 | 1.414 | 1.416 | 1.405 | 1.412 |
| 1.600 | 1.279 | 1.280 | 1.283 | 1.281 |
| 1.800 | 1.151 | 1.157 | 1.157 | 1.155 |
| 2.000 | 1.043 | 1.049 | 1.052 | 1.048 |
| 2.500 | 0.766 | 0.772 | 0.769 | 0.770 |
| 3.000 | 0.523 | 0.525 | 0.526 | 0.524 |
| 3.500 | 0.350 | 0.349 | 0.349 | 0.349 |
| 4.000 | 0.263 | 0.263 | 0.263 | 0.263 |
| 5.000 | 0.183 | 0.182 | 0.182 | 0.183 |
| 6.000 | 0.140 | 0.141 | 0.140 | 0.141 |
| 7.000 | 0.103 | 0.103 | 0.103 | 0.103 |

## BIBLIOGRAPHY

[1] R.A. Tawil, *Phys. Rev.* **B11**, 4891 (1975)

[2] C.S. Wang and J. Callaway, *Phys. Rev.* **B11**, 2417 (1975)

[3] For excellent reviews of this topic reference is made to articles by:
M.J. Cooper, *Advan. Phys.* **20**, 453 (1971), and I.R. Epstein, *Accts. Chem. Research* **6**, 145 (1973)

[4] R.A. Tawil and S.R. Langhoff *J. Chem. Phys.* 4, 1972 (1975); 6, 2745 (1975)

[5] W. Phillips and R.J. Weiss, *Phys. Rev.* **171**, 790 (1968).

[6] P. Kaijser, P. Lindner, A. Andersen, and E. Thulstrup, *Chem. Phys. Letters* **23**, 409 (1973).

[7] S. Manninen and T. Paakkari, *Phys. Fenn.* **9**, 129 (1974).

[8] P. Eisenberger and W.A. Reed, *Phys. Rev.* **B9**, 3242 (1974).

[9] R.A. Tawil and S.P. Singhal , *Phys. Rev.* **B11**, 699 (1975).

[10] W.Y. Ching and J. Callaway, *Phys. Rev.* **B** (to be published).

[11] R.A. Tawil and J. Callaway, *Phys. Rev.* **B7**, 4242 (1973).

[12] J. Rath and J. Callaway *Phys. Rev.* **B8**, 5398 (1973).

[13] J. Southworth and P. Deleeuv, *Digital Computation and Numerical Methods*, McGraw-Hill, 483 (1965).

[14] S. Manninen, T. Paakkari and K. Kajantie, *Philos. Mag.* **29** 167 (1974)

[15] M. Cooper P. Pattison, B. Williams, and K.C. Pandaey, *Philos. Mag.* **29**, 1237 (1974).

[16] The nomenclature adopted here is due to: C.O. Larson and W.L. Gordon, *Phys. Rev.* **165**, 703 (1967).

**Reference Code for AJSE Information Retrieval : QC 1276 TA1. Paper received November 11, 1975.**